

SEMA AKYALCIN<sup>1</sup>  
LEVENT AKYALCIN<sup>1</sup>  
MORTEN BJØRGEN<sup>2</sup>

<sup>1</sup>Department of Chemical Engineering, Faculty of Engineering, Eskisehir Technical University, Eskisehir, Turkey

<sup>2</sup>Department of Life Sciences and Health, Faculty of Health Sciences, Oslo Metropolitan University, Oslo, Norway

SCIENTIFIC PAPER

UDC 547:66:549.67

## CATALYTIC PERFORMANCE OF DESILICATED HZSM-12 FOR BENZYLATION REACTION OF BENZENE WITH BENZYL ALCOHOL

### Article Highlights

- In the benzylation reaction, desilicated HZSM-12 showed better catalytic activity than HZSM-12
- The effects of reaction parameters were investigated
- The organic species deposited on the catalyst decreased the activity of the desilicated HZSM-12

### Abstract

The catalytic production of diphenylmethane from the reaction of benzene with benzyl alcohol was investigated using HZSM-12 and desilicated HZSM-12 that was obtained by treating ZSM-12 with 0.2M NaOH solution at 85 °C for 60 min. The untreated and alkaline treated ZSM-12 zeolites were characterized by X-ray diffraction, nitrogen adsorption/desorption isotherms, scanning electron microscopy, inductively coupled plasma optical emission spectrometry, and temperature-programmed desorption of ammonia. The desilicated HZSM-12 showed promising catalytic performance with benzyl alcohol conversion of 100% and the selectivity to diphenylmethane of 74% and 87% in 4 h and 8 h reaction time, respectively. The reaction parameters affecting benzyl alcohol conversion and product distribution were also presented. The activities of fresh and regenerated catalysts were compared, and characterization results indicated that the occluded organic molecules decreased the number of acidic sites of the catalyst after the reaction and regeneration.

**Keywords:** benzyl alcohol, benzylation, catalyst deactivation, desilication, diphenylmethane, ZSM-12.

The benzylated aromatics are produced via the reaction of benzene (B) with benzyl alcohol (BA) or benzyl chloride [1,2]. An essential chemical compound obtained from the benzylation of benzene is diphenylmethane (DPM), and it is used as a fixative and a scenting soap in the fragrance industry, a plasticizer for dyes, and a synergist in some insecticides [2,3]. DPM is also employed to improve the thermal stability

of polyester and the stability and lubricating properties of jet fuels [2,3]. During the synthesis of DPM, using less reactive benzyl alcohol instead of benzyl chloride as a benzylation agent is an eco-friendly process since the formation of HCl as a by-product is avoided [4]. The benzylation reaction pathway in the presence of the catalyst [1] is given in Figure 1.

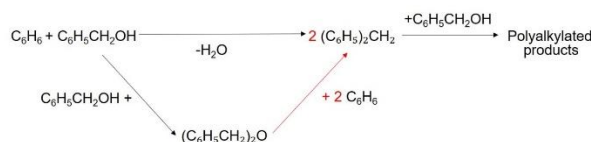


Figure 1. Benzylation reaction pathway of benzene with benzyl alcohol.

The benzylation reaction also forms dibenzyl ether (DBE) and polyalkylated products (PAB). Therefore, choosing the proper catalyst for the reaction is

Correspondence: S. Akyalcin, Department of Chemical Engineering, Eskisehir Technical University, 26555, Eskisehir, Turkey.

E-mail: [sdogruel@eskisehir.edu.tr](mailto:sdogruel@eskisehir.edu.tr)

Paper received: 20 June, 2022

Paper revised: 23 February, 2023

Paper accepted: 17 March, 2023

<https://doi.org/10.2298/CICEQ220620006A>

essential, which maximizes the selectivity of the desired monobenzylated aromatics. Additionally, benzyl alcohol usage instead of benzyl chloride requires a stronger acid catalyst having good catalytic activity [2,4].

Benzylation reactions are generally performed in the presence of homogeneous acid catalysts such as  $\text{AlCl}_3$ ,  $\text{FeCl}_3$ , and  $\text{H}_2\text{SO}_4$  [5]. These catalysts cause several problems: difficulty separating and recovering the catalyst and corrosion problems. Therefore, replacing these homogeneous catalysts with heterogeneous catalysts is highly desirable.

In benzylation reactions, zeolites such as H-Beta, Mordeinite, HY, and HZSM-5 are used as heterogeneous catalysts due to their strong acidity, large surface area, and stable porous structure [2,6–9]. However, the catalytic performance of zeolites can be limited because of their microporous channel structure. The reduction of particle size from the micrometer to the nanometer scale and the formation of mesopores in zeolite by post-synthesis treatments improve accessibility and molecular transport in catalysis [10,11]. Among the post-synthesis treatment, desilication is a widely applied preparation method to prepare mesoporous zeolites due to the combination of efficiency and simplicity [11,12].

Leng *et al.* [1] prepared hierarchical mordenites using a sequential post-treatment method based on a commercial mordenite with a Si/Al molar ratio of 15. They report that acid-base-acid-leached mordenite exhibited the highest catalytic activity, with a BA conversion of 99.6%, compared to untreated mordenite (BA conversion of 6.1%), acid-leached mordenite (BA conversion of 40.2%), and acid-base-leached mordenite (BA conversion of 28.8%) under the same reaction conditions in the benzylation of benzene with benzyl alcohol [1]. They stated that the enhanced catalytic performance was attributed to more accessible acid sites and much better mass transfer ability from rich mesoporosity in acid-base-acid-leached mordenite [1]. Wang *et al.* [6] prepared the hierarchical Beta by base treatment of a commercial Beta with a Si/Al molar ratio of 12.5. They report that the desilicated catalyst exhibited much poorer catalytic activity than the untreated catalyst due to the significant loss of total acidity [6]. They state that the subsequent acid treatment after desilication can significantly recover zeolite Beta's acidity and improve the desilicated Beta's catalytic performance in some acid-catalytic reactions [6]. Wang *et al.* [13] synthesized mesoporous aluminosilicates (ZM) by assembling zeolitic subunits obtained by the controllable desilication of nano-sized ZSM-5 zeolite particles in  $\text{Na}_2\text{SiO}_3$  aqueous solution, with cetyltrimethylammonium

m bromide (CTAB) as the template. They report that ZM possessed a mesoporous structure similar to MCM-41, and ZSM-5 subunits were present in the pore walls [13]. They state that HZM exhibited much higher catalytic activity with a BA conversion of 78% than HAI-MCM-41 (BA conversion of 21%) and HZSM-5 (BA conversion of 8%) in 10 h reaction time under the same reaction conditions in the liquid phase benzylation of benzene with benzyl alcohol [13]. Candu *et al.* [2] investigated the liquid phase benzylation of benzene to diphenylmethane over various catalysts (mordenite and beta zeolites with Si/Al of 10.8 and 35.8). They report that the observed difference in the BA conversion for Beta zeolite (Si/Al=10.8) and mordenite (Si/Al=10.0), whose Si/Al molar ratio is close to each other, is quite low (48.4% for Beta zeolite versus 44.5% for mordenite) while the selectivity to DPM was 30.9% for Beta zeolite and 3.1% for mordenite. However, the BA conversion on Beta zeolite (Si/Al = 35.8) was almost 66% with 22% DPM selectivity. They stated that both the activity and selectivity were affected by the Si/Al molar ratio for both zeolites, and a higher Si/Al molar ratio was found to allow an increased benzyl alcohol conversion. The conversion of BA and product distribution largely depends on the zeolite nature and the experimental conditions [2].

ZSM-12 zeolite is a desirable catalyst for the petrochemical industry, including alkylation of benzene with propene [14], disproportionation of alkyl aromatic hydrocarbons [15], cracking, hydrocracking [16], isomerization reactions [17], and other petroleum refining processes [16]. ZSM-12 can potentially apply in catalysis due to their unidirectional twelve-membered ring linear channel system and strong acidic character [18]. Akyalcin *et al.* [19] prepared the mesoporous ZSM-12 samples by desilication of ZSM-12 under various NaOH concentrations (0.2 M, 0.4 M, and 0.6 M) at different temperatures (35 °C, 65 °C, and 85 °C) and treatment times (15 min, 30 min, and 60 min), and Taguchi's design of experiment was applied to investigate the influence of desilication parameters. They report that the zeolite treated with 0.2 M NaOH at 85 °C for 60 min shows higher catalytic activity than the other desilicated samples in the benzylation of benzene to diphenylmethane under constant reaction conditions [19].

This study assessed the catalytic performances of HZSM-12 and desilicated HZSM-12 in the benzylation reaction of benzene with environmentally friendly benzyl alcohol as an alkylating agent. The effects of reaction temperature, catalyst loading, and benzene to benzyl alcohol molar ratio on conversion and the selectivity of DPM, DBE, and PAB were determined. Additionally, the reusability of the desilicated HZSM-12

was tested. XRD and NH<sub>3</sub>-TPD characterized the fresh, spent, and regenerated samples to evaluate the impact of deactivation and regeneration on the properties of the catalyst.

## MATERIAL AND METHODS

### Catalyst synthesis

ZSM-12 was hydrothermally synthesized with LUDOX HS-40 colloidal silica (40 wt.%, Sigma Aldrich), sodium aluminum oxide (Sigma Aldrich, technical grade), tetraethylammonium hydroxide (TEAOH, 35 wt.%, Aldrich), and deionized water according to the method proposed by Gopal *et al.* [20] and Hou *et al.* [21]. The gel prepared with the composition of Na<sub>2</sub>O: Al<sub>2</sub>O<sub>3</sub>: 80 SiO<sub>2</sub>:12.7 TEAOH: 1040 H<sub>2</sub>O was transferred into a 125 mL Parr Teflon lined autoclave, and the zeolite was crystallized at 160 °C for 5.5 days. Thus, the solid product was filtered, washed with deionized water, and dried at 100 °C overnight. The as-synthesized zeolite was calcined in static air at 520 °C for four hours to remove the template.

The calcined zeolite was treated in 0.2 M NaOH solution (in the proportion of 20 mL/g) at 85 °C for 60 minutes, and then it was filtered, washed with deionized water, and dried overnight at room temperature. After that, the zeolite samples (ZSM-12 and desilicated ZSM-12) were ion exchanged three times with a fresh 1 M NH<sub>4</sub>NO<sub>3</sub> (in the proportion of 20 mL/g) for two hours at 75 °C, followed by calcination at 520 °C for four hours. The final H-form of ZSM-12 and desilicated ZSM-12 were labeled as HZSM-12 and desilicated HZSM-12.

### Catalyst characterization

The X-ray powder diffraction (XRD) patterns of the samples were collected on a Rigaku MiniFlex 600 Diffractometer using a CuK $\alpha$  X-ray source (40 kV, 15 mA). The XRD analysis was carried out from 5° to 40° 2 $\theta$  at a scanning rate of 1.2°/min.

Nitrogen adsorption/desorption isotherms were measured at 77 K on a Quantachrome Autosorb IQ-MP-XR instrument to determine the textural properties of the samples. The samples were outgassed in a vacuum at 200 °C for four hours before measurements.

The elemental compositions of the catalysts were determined by inductively coupled plasma optical emission spectrometry (ICP-OES) in a Perkin-Elmer Optima 4300DV device.

Scanning electron microscope (SEM) images of the samples coated with a gold layer were obtained using Zeiss Supra 50 VP microscope.

The acidic behavior of the samples was

determined by NH<sub>3</sub>-TPD measurements, which were accomplished on a Quantachrome Autosorb IQ-Chemi-XR instrument. For the analysis, the sample was pre-treated in helium flow at 500 °C for two hours to remove moisture. The sample was then cooled to 100 °C and saturated with pure ammonia flow for 30 min. After the adsorption, physisorbed ammonia was purged using helium flow at 100 °C for 60 min. Finally, the NH<sub>3</sub>-TPD profile was recorded under helium flow (30 mL/min) by heating the sample from 100 °C to 600 °C at a ramp rate of 10 °C/min.

The thermogravimetric analyses (TGA) of the fresh and spent catalysts were conducted on a Perkin Elmer STA 6000 instrument heated from 30 °C to 900 °C (10 °C/min) under airflow (50 mL/min).

### Catalytic activity test

Under solvent-free conditions, the benzylation reaction was performed in a laboratory-scale reactor described previously [19,22]. The experiments were conducted at different reaction temperatures of 60 °C–80 °C, catalyst loading of 0 mg/mL–4.9 mg/mL, and benzene to benzyl alcohol molar ratio of 21/1 to 98/1. In a typical experiment, benzene was placed in the reactor, heated, and magnetically stirred. When benzene reached the desired temperature, a fresh catalyst and benzyl alcohol (BA) were added to the reactor. Then the first sample was taken from the reactor to determine the initial composition of the reaction mixture. The samples taken at different time intervals from the reactor were put into the centrifuge tubes in an ice bath and then centrifuged to separate the catalyst from the samples. The samples were analyzed using Agilent HP 7890 gas chromatography, equipped with FID and HP-5 column. The following temperature program was employed: isothermal at 50 °C for 2 min, heating at 20 °C/min to 250 °C, and isothermal at 250 °C for 6 min. Quantification of B, BA, DPM, and DBE was done using the internal standard calibration method. The amount of PAB was calculated using reaction stoichiometry (Figure 1). The product selectivity was determined as the moles of product formed divided by the moles of benzyl alcohol reacted.

## RESULTS AND DISCUSSION

### Catalyst characterization

The XRD patterns of HZSM-12 and desilicated HZSM-12 samples are shown in Figure 2. All of the peaks observed at 7.4°, 8.8°, 20.8°, and 23.1° of 2 $\theta$  are attributed to the phases of the ZSM-12 zeolite [16,19–21].

XRD peak positions of the desilicated HZSM-12 are very close to that of HZSM-12. Figure 2 shows that

although the crystal structure of the sample is preserved after alkali treatment, the peak intensities of the desilicated HZSM-12 decrease slightly due to the removal of Si from the zeolite framework, in accord with Wei and Smirniotis [23].

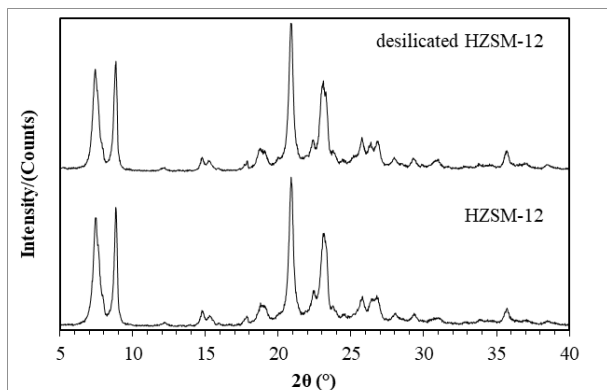


Figure 2. XRD patterns of HZSM-12 and desilicated HZSM-12.

The SEM images for HZSM-12 and desilicated HZSM-12 are shown in Figure S1. The zeolite samples consist of about 1  $\mu\text{m}$  crystallites. HZSM-12 agglomerates are formed by nanocrystals with sizes determined by the Scherrer equation [24] of about 22 nm. These findings are compatible with the reports given in the literature [20,21,25]. As seen in Figure S1, there are no significant differences among the samples.

The  $\text{N}_2$  adsorption/desorption isotherms and pore size distribution curves of HZSM-12 and desilicated HZSM-12 are given in Figure S2.  $\text{N}_2$  adsorption/desorption measurement for the HZSM-12 resulted in a type I isotherm, indicating a microporous material [26] with a narrow hysteresis loop between 0.4 and 0.8 that implies the presence of some mesoporosity. The presence of mesopores in HZSM-12 with a mean pore diameter of about 4.3 nm (Figure S2) could be generated due to voids between the nanocrystals that form the agglomerates [25]. On the other hand, the  $\text{N}_2$  adsorption/desorption isotherm of the desilicated HZSM-12 represents type I and type IV behavior with the rather pronounced hysteresis loop. Those are associated with capillary condensation in the mesopore structure [26]. As seen in Figure S2, the desilicated HZSM-12 shows a bimodal mesopore distribution with mean diameters of 6.5 nm and 9.5 nm. The results of  $\text{N}_2$  adsorption and desorption analysis are given in Table 1.

As seen from Table 1, the desilicated HZSM-12 shows a lower micropore volume ( $0.06 \text{ cm}^3/\text{g}$ ) than HZSM-12 ( $0.11 \text{ cm}^3/\text{g}$ ), which is also in compliance with the slight crystallinity loss observed by XRD. The decrease in micropore volume is coupled with increased external surface area ( $127 \text{ m}^2/\text{g}$  to  $146 \text{ m}^2/\text{g}$ ) and mesopore volume ( $0.11 \text{ cm}^3/\text{g}$  to  $0.26 \text{ cm}^3/\text{g}$ ).

Alkaline treatment of ZSM-12 leads to a significant increase in mesopore formation, resulting from the preferential dissolution of Si from the zeolite framework [27,28]. Indeed, ICP-OES analysis results show that the alkaline treatment of ZSM-12 leads to the preferential removal of silicon from the zeolite lattice.

Table 1. Elemental composition and  $\text{N}_2$  sorption characteristics of the samples.

Sample	HZSM-12	Desilicated HZSM-12
Si/Al <sup>a</sup>	40.8	32.9
$S_{\text{BET}}$ ( $\text{m}^2/\text{g}$ )	384	338
$S_{\text{ext}}^{\text{b}}$ ( $\text{m}^2/\text{g}$ )	127	146
$S_{\text{micro}}^{\text{b}}$ ( $\text{m}^2/\text{g}$ )	257	192
$S_{\text{meso}}^{\text{c}}$ ( $\text{m}^2/\text{g}$ )	64	127
$V_{\text{micro}}^{\text{b}}$ ( $\text{cm}^3/\text{g}$ )	0.11	0.06
$V_{\text{meso}}^{\text{c}}$ ( $\text{cm}^3/\text{g}$ )	0.11	0.26
$V_{\text{total}}^{\text{d}}$ ( $\text{cm}^3/\text{g}$ )	0.25	0.37

<sup>a</sup>ICP-OES; <sup>b</sup>t-Method; <sup>c</sup>BJH Method (adsorption branch); <sup>d</sup>Volume absorbed at  $p/p_0=0.99$ .

$\text{NH}_3$ -TPD was used to determine the strength and number of the acidic sites of HZSM-12 and desilicated HZSM-12. Two desorption peaks characterize the  $\text{NH}_3$ -TPD profiles of the samples given in Figure S3; a low-temperature peak below  $300 \text{ }^\circ\text{C}$  and a high-temperature peak at  $300 \text{ }^\circ\text{C}$ – $550 \text{ }^\circ\text{C}$ . The low-temperature peak is assigned to the weak acidic sites, commonly attributed to silanol groups at the external surface or in lattice defects, and OH groups bonded to extra-framework aluminum species [29]. The high-temperature peak has been attributed to  $\text{NH}_3$  adsorbed on the strong acid sites generated by framework tetrahedral aluminum species [29]. The quantities of weak and strong acid sites were determined by integrating the area under each peak shown in Figure S3; the results are given in Table 2.

Table 2. Amount of acid sites for the samples.

Sample	Amount of acid sites (mmol/g)		
	Weak	Strong	Total
HZSM-12	0.39(206.1)*	0.31(406.9)*	0.70
Desilicated HZSM-12	0.47 (178.9)	0.28 (387.4)	0.75
Spent catalyst	0.46 (172.1)	0.07 (348.6)	0.53
Regenerated catalyst	0.46 (181.1)	0.13 (387.4)	0.59

\* $T_{\text{max}}$  is given in parenthesis

The results given in Table 2 show that the number of weak acidic silanol groups increases due to the alkaline treatment of ZSM-12. Although the number of strong acidic sites remains virtually unchanged, the high-temperature peak is shifted to the lower temperature due to the lower intrinsic acidity of the Brønsted sites [30]. ICP-OES analysis of the samples shows that the desilicated HZSM-12 contains more aluminum than HZSM-12, and the Si/Al ratios of ZSM-12 samples decreased from 40.8 to 32.9 after the alkaline treatment of ZSM-12. The results of ICP-OES and  $\text{NH}_3$ -TPD analyses show that the geometric arrangement of aluminum atoms in the zeolite framework affects the acidity of the catalyst. It was

reported that, during the alkali treatment, some framework aluminum species responsible for forming the strong acid sites were re-distributed as extra-framework aluminum species due to the leaching of the framework siliceous species [31–33]. However, our previous study shows that the mesopores obtained in the specified desilication condition were successfully introduced without decreasing the strong Brønsted acidity [19]. Svelle *et al.* [34] stated that the mode of mesopore formation, i.e., concerning where and to which extent the alkaline solution attacks each zeolite particle, is elusive. They demonstrated that the mesopore formation according to both the Al-directed dissolution of siliceous areas and selective dissolution or etching along boundaries, intergrowths, and defects within each particle is important [34].

### Catalytic activity

Catalytic performances of HZSM-12 and desilicated HZSM-12 were evaluated by the benzylation reaction of benzene with benzyl alcohol at 80 °C, 56/1 molar ratio of B to BA, and 2.5 mg/mL of catalyst loading. The conversion of benzyl alcohol over HZSM-12 and desilicated HZSM-12 is shown in Figure 3.

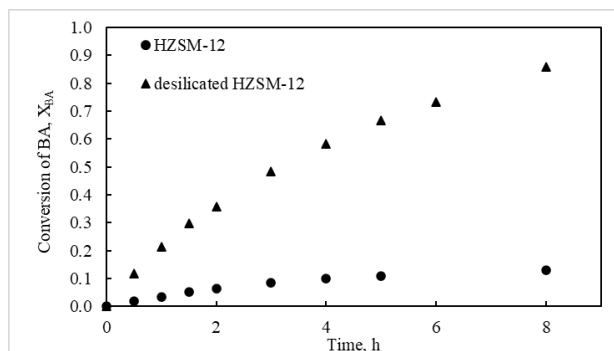


Figure 3. Catalytic activities of HZSM-12 and desilicated HZSM-12 in the benzylation reaction of benzene with benzyl alcohol at 80 °C, 2.5 mg/mL of catalyst loading, and 56/1 molar ratio of B to BA.

As shown in Figure 3, the alkaline-treated catalyst sample shows substantially higher catalytic activity than the untreated ZSM-12. To explain why the desilicated HZSM-12 exhibited higher catalytic activity in the reaction, the relationship between the structural properties and the catalytic performances of the catalyst needs to be discussed. It is known that ZSM-12 has a one-dimensional channel system with a 12-membered ring pore channel of 0.57 nm x 0.61 nm [19,21]. The molecular size of benzene (0.5 nm), benzyl alcohol (0.7 nm), DPM (0.9 nm), and DBE (1.2 nm) is close to or larger than the pore size of untreated ZSM-12 [35]. Such a pore size is inadequate for mass transfer to increase the conversion of BA into DPM. In the benzylation of benzene with benzyl alcohol, two

reaction step is proposed to form DPM (Figure 1): (1) the direction formation of DPM by the alkylation of benzene with benzyl alcohol; (2) the conversion of DBE formed by the self-condensation of benzyl alcohol to DPM. Therefore, mass transfer ability is an important factor that affects the catalytic performance of the catalyst. As listed in Table 1, the desilicated HZSM-12 has a higher mesopore volume and external surface area than HZSM-12. Additional mesopores and external surface area will likely improve the mass transfer ability. Furthermore, the accessibility of acid sites is naturally vital in this reaction. The catalyst performs better in the benzylation reaction with higher mass transfer ability and more accessible acid sites. These results comply with the literature findings [1,6,8,19]. Akyalcin *et al.* [19] stated that ZSM-12, treated with 0.2 M NaOH at 85 °C for 60 min, exhibits a 10-fold enhancement of the catalytic activity compared to microporous HZSM-12 for the benzylation reaction of benzene with benzyl alcohol. In this study, the difference in the catalytic performance of the desilicated HZSM-12 can be explained by the strength of strong acid sites of the catalyst since the stronger acid sites are required to polarize benzyl alcohol into an electrophile that attacks the benzene ring [2]. When the maximum temperature ( $T_{max}$ ) for the  $NH_3$  desorption peak of the samples given in Table 2 is investigated, the shift of the second peak to a lower temperature for desilicated HZSM-12 indicates a decrease in the acid strength of the strong acid sites. This case leads to somewhat lower catalytic activity in converting benzyl alcohol to diphenylmethane. Milina *et al.* [36] stated that both compositional and porosity variations induced by alkaline treatment contribute to the catalytic performance of desilicated ZSM-5 in the liquid phase alkylation of toluene with benzyl alcohol. Svelle *et al.* [34] stated that the comparison of catalyst performance between mesoporous samples of ZSM-5 in the methanol to hydrocarbons reaction is not straightforward, as the Si/Al ratio, distribution of intergrowths/defects, mesoporosity, particle size, and other characteristics influence activity and deactivation rates in an interdependent manner. Consequently, the catalytic performance of the catalyst for the reaction of benzene with benzyl alcohol could be attributed to the synergic effect of mass transfer efficiency and surface acidity.

The effects of reaction parameters (reaction temperature, catalyst loading, and benzene to benzyl alcohol molar ratio) on the BA conversion and the DPM, DBE, and PAB selectivity were investigated using desilicated HZSM-12.

### Effect of reaction temperature

Investigation to the effect of reaction temperature

on the reaction rate, the benzylation reaction was performed at 60 °C, 70 °C, 75 °C, and 80 °C, with 3.9 mg/mL of catalyst loading and 56/1 molar ratio of B

to BA. The results are shown in Figure 4a.

As shown in Figure 4a, the influence of reaction temperature on the BA conversion is quite strong.

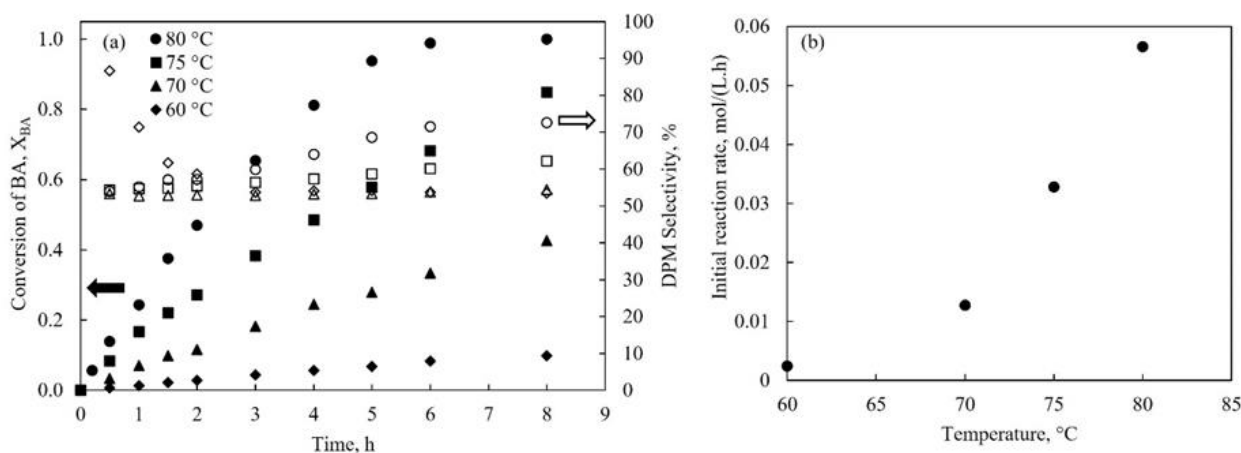


Figure 4. Effect of reaction temperature (a) on the benzyl alcohol conversion and DPM selectivity (b) on the initial reaction rate (3.9 mg/mL of catalyst loading, 56/1 molar ratio of B to BA).

The initial reaction rate shown in Figure 4b was calculated from Eq. 1 using a conversion of less than 10%, and the reaction rate can be considered a linear function of time.

$$-r_{BA_0} = C_{BA_0} \frac{X_{BA}}{t} \quad (1)$$

Figure 4b indicates that the reaction rate increases exponentially with the temperature, indicating that external and internal diffusion resistances can be neglected during the reaction since a chemical change is more temperature sensitive than a physical change [37]. Increasing the reaction temperature led to increased BA conversion, which increased the selectivity to DPM. For example, at 70 °C, the BA conversion was 24% after a reaction time of 4 h; at 80 °C, the BA conversion reached 81%. Therefore, the selectivity to DPM increased from 53% to 64%, paralleling the BA conversion. When the reaction time at 80 °C was increased from 4 h to 8 h, the selectivity to DPM was increased from 64% to 73%. However, at the same conversion, the change in the reaction temperature did not prominently change (~1%) in the selectivity to DPM. Therefore, 80 °C was suggested as the optimal reaction temperature under the atmospheric pressure by considering the obtained conversion and selectivity for the benzylation of benzene with benzyl alcohol in the presence of desilicated HZSM-12.

#### Effect of catalyst loading

The effect of catalyst loading on the reaction rate was investigated by performing the reaction in the

presence of desilicated HZSM-12 at 0 mg/mL–4.9 mg/mL of varying catalyst loadings, 56/1 molar ratio of B to BA, and  $T=80$  °C. The results are given in Figure 5a.

Figure 5a indicates that the conversion of BA increases with an increase in the catalyst loading. The initial reaction rate,  $-r_{BA_0}$ , versus catalyst loading, is given in Figure 5b. As can be seen in Figure 5b, the initial reaction rate linearly increases with catalyst loading, as expected, since the active sites of the catalyst are proportional to the amount of catalyst, and the mathematical expression can be given by:

$$-r_{BA_0} (\text{mol} / \text{L} \cdot \text{h}) = 0.0152 C_{cat} (\text{mg} / \text{mL}) \quad (2)$$

When the reaction was carried out without a catalyst, no conversion was observed at a reasonable time. Thus, the reaction rate was considered negligible without the catalyst. This result is compatible with the report by Narender *et al.* [38]. The effect of catalyst loading on the BA conversion and product selectivities for 4 h and 8 h reaction time was given in Figure 5c.

Figure 5c indicates that the formation of DPM increases with DBE consumption, and PAB was also formed during the reaction. When the catalyst loading increased from 2.5 mg/mL to 4.9 mg/mL for 4 h reaction time, the BA conversion increased from 58% to 98%, and the selectivity towards DPM increased from 55% to 69%, paralleling the BA conversion. Under the same reaction conditions, the DPM and PAB selectivities increased with a longer reaction time. After 8 h reaction time, the DPM and PAB selectivities were 78% and 7%, respectively. The results show that the increase in the

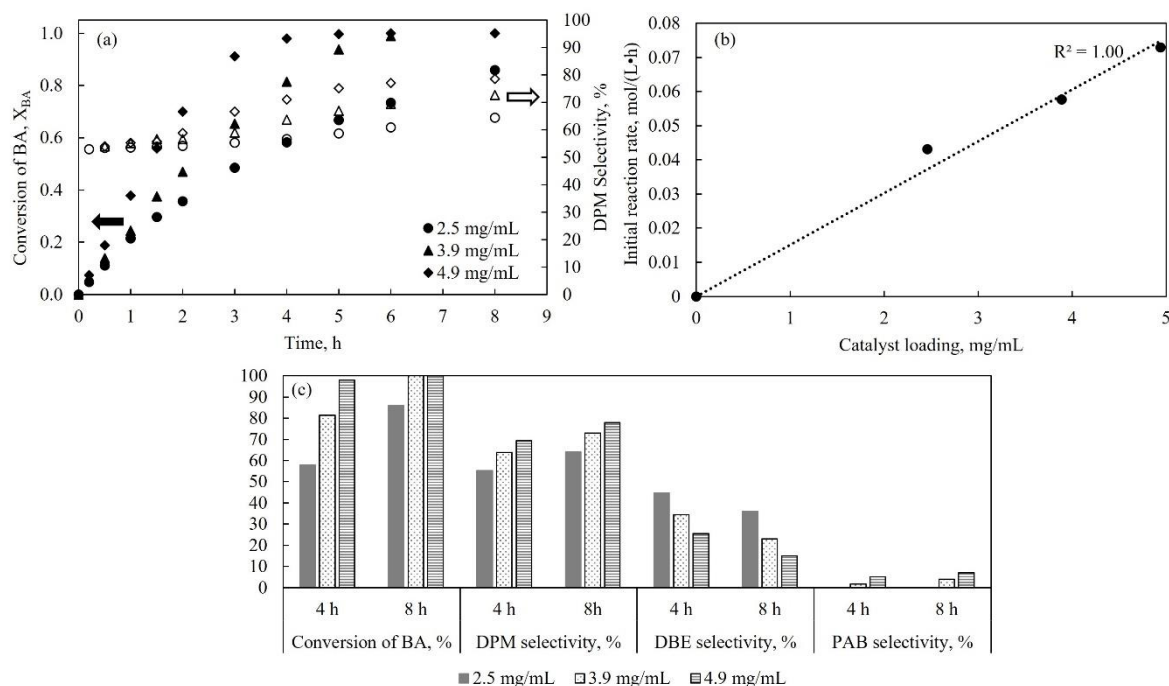


Figure 5. Effect of catalyst loading (a) on the BA conversion and DPM selectivity (b) on the initial reaction rate at 80 °C, and 56/1 molar ratio of B to BA (c) on the BA conversion and product selectivities for 4 h and 8 h reaction time at 80 °C, 56/1 molar ratio of B to BA.

catalyst loading did not significantly change the selectivity to DPM at the same conversion since increasing the catalyst loading provides the same effect on the rate of side reactions (Figure 1). Therefore, further experiments were performed with low catalyst loading (2.5 mg/mL) to reduce PAB formation.

#### Effect of benzene to benzyl alcohol molar ratio

The benzylation reactions were carried out at B to BA molar ratios of 21/1, 56/1, and 98/1 while maintaining 2.5 mg/mL of catalyst loading and the reaction temperature at 80 °C. The effects of the B to BA molar ratio on the BA conversion are given in Figure 6a.

Figure 6a shows that increasing the molar ratio of

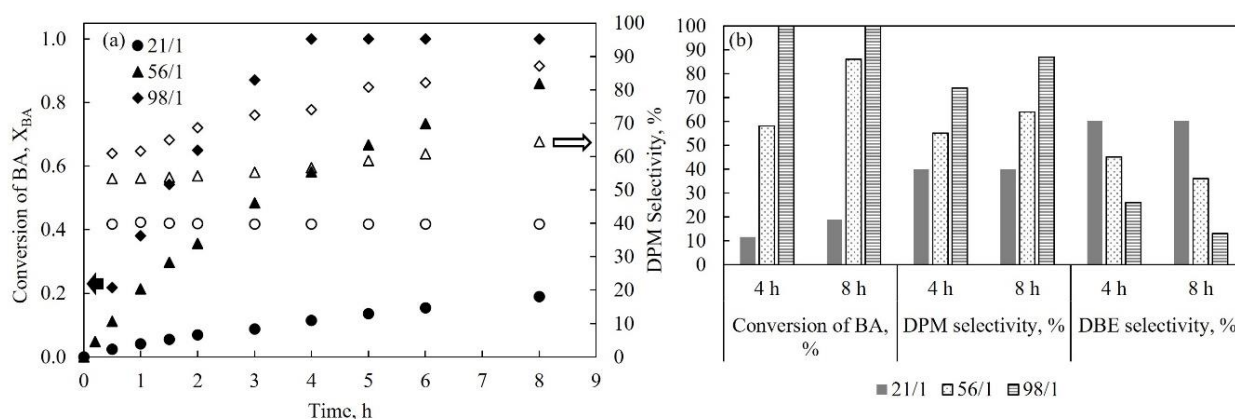


Figure 6. Effect of B to BA molar ratio (a) on the BA conversion and DPM selectivity (b) product selectivities at 80 °C, and 2.5 mg/mL of catalyst loading.

### Catalyst reusability and deactivation

After completion of the benzylation reaction, the catalyst was filtered from the reaction mixture and dried. This catalyst was denoted as a "spent catalyst." Before reusing this catalyst in the benzylation reaction, the spent catalyst was calcined at 520 °C for four hours under static air. The obtained catalyst was named a "regenerated catalyst." The reaction was performed at 80 °C and 56/1 molar ratio of B to BA in the presence of the regenerated catalyst with 2.5 mg/mL of catalyst loading to compare the catalytic activity of the fresh and regenerated catalyst. The conversion of benzyl alcohol dropped from 86% (fresh catalyst) to 45% (regenerated catalyst) for 8 h reaction time, while the DPM selectivity varies from 64% (fresh catalyst) to 56% (regenerated catalyst). The change of the acidic sites of the catalyst after regeneration can explain this activity difference. To determine the differences in the acid amount and the acid strength of the fresh, spent, and regenerated catalysts, the NH<sub>3</sub>-TPD profiles given in Figure S4 were obtained. Table 2 indicates that after the eight hours reaction time of the fresh catalyst, the total acid sites on the catalyst significantly reduced, and a higher loss of strong acid sites occurred, which means that strong acid sites are more active in the benzylation of benzene with benzyl alcohol. Yoo and Smirniotis [39] stated that ZSM-12 was deactivated due to site coverage during the alkylation of isobutene with 2-butene at 80 °C and 300 psig. In this study, the occluded organic species formed on the catalyst during the reaction deactivated the catalyst, as was confirmed by the TGA analysis shown in Figure 7. From the recorded profiles, the weight loss before 200 °C is attributed to the desorption of the adsorbed water, and the weight loss of 4.5 wt% between 200 °C and 400 °C is associated with the desorption/decomposition of adsorbed organic compounds generated during the reaction. The weight loss of 5.5 wt% above 400 °C is attributed to the decomposition/oxidation of larger-sized organic molecules generated during the reaction [40,41].

Kim *et al.* [40] stated that the conventional zeolite deactivated rapidly in the liquid phase Friedel Craft alkylation reactions due to the deposition of carbon residue and/or water inside the micropores or the external surfaces. They also report that various poly-alkylated aromatic compounds generated via side reactions, i.e., self-condensation of benzyl alcohol or the benzylation of benzene, and their repetition, block the access of reactants into the active sites [40]. The spent catalyst was regenerated by the calcination method to maintain the catalytic performance. The number of acid sites of the regenerated catalyst given in Table 2 showed that the acidic sites of the spent catalyst were partially recovered. The strong acid sites of the regenerated catalyst recovered to 0.13 mmol/g,

which accounted for 46% of the fresh catalyst. Two factors can explain the significant reduction of acidic sites of the catalyst after regeneration. One of them is high-temperature calcination for regeneration, which leads to the steaming of the zeolite, and, thus, the formation of some defects that dehydroxylate at high temperatures [41,42]. The other one is that the calcination temperature in this work was only 520 °C and did not reach 700 °C shown in Figure 7, to remove some organic species' residue. Corroborating the thermal stability of the zeolite samples [25,43], the XRD patterns of the fresh, spent, and regenerated catalyst given in Figure 8 were also investigated.

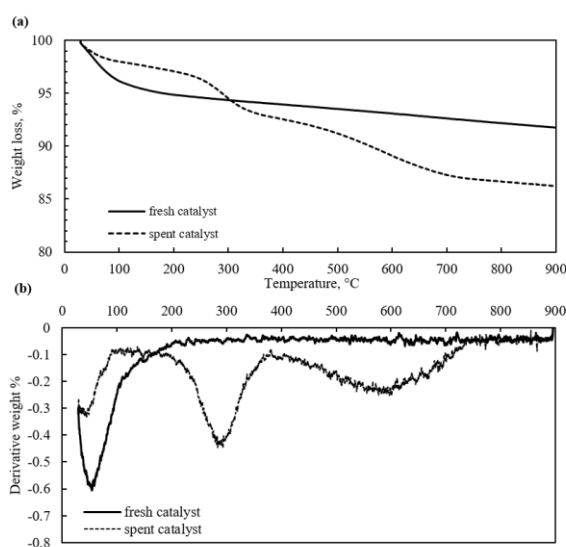


Figure 7. (a) TG and (b) DTG profiles of the fresh and spent catalysts.

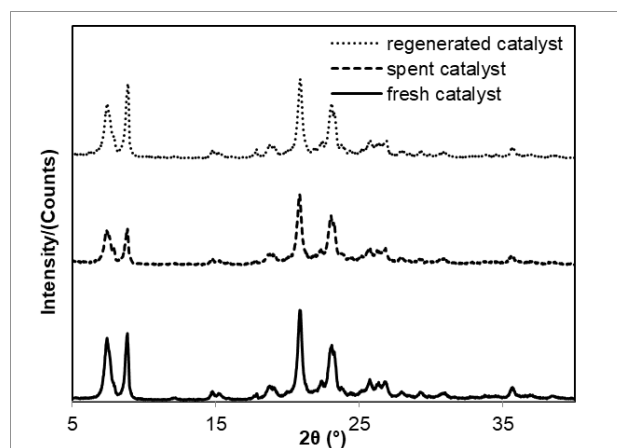


Figure 8. The XRD patterns of the fresh, spent, and regenerated catalysts.

The results indicated that although the spent and regenerated catalyst retains the crystal structure of MTW, the peak intensities of the samples are different. When the relative crystallinity was calculated from the intensities of the peaks at 7.4°, 8.8°, 20.8°, and 23.1° relative to the fresh catalyst, the relative crystallinities



of the spent and regenerated catalysts were found to be 69% and 95%, respectively. After calcinating the spent catalyst, the catalyst almost recovers the original crystallinity.

## CONCLUSION

The benzylation reaction of benzene with benzyl alcohol was performed over HZSM-12 and desilicated HZSM-12. The increased mesoporosity of ZSM-12 via alkaline treatment enhanced the catalytic activity of ZSM-12. The effects of reaction parameters on the benzyl alcohol conversion and product selectivities were studied in the presence of desilicated HZSM-12, and selectivity to DPM of 74% for 100% BA conversion was achieved in 4 h of reaction time at 80 °C, 98/1 molar ratio of B to BA, and 2.5 mg/mL of catalyst loading. Under the same reaction conditions, the DPM selectivity was 87% in 8 h reaction time. The catalyst's reusability was investigated after calculating the spent catalyst in static air at 520 °C for four hours. Although the diffractograms of the desilicated HZSM-12 samples (fresh, spent, and regenerated samples) have proven that there were no structural changes, the NH<sub>3</sub>-TPD results show that the coverage of the acid sites resulting from organic species produced during the reaction caused deactivation of the catalyst. However, the desilicated HZSM-12 can be regarded as a promising heterogeneous catalyst to improve the selectivity of diphenylmethane by using less reactive benzyl alcohol instead of benzyl chloride as a benzylation agent.

## ACKNOWLEDGMENT

This work was supported by Anadolu University, Scientific Research Project Commission under grant number 1410F412, and Eskisehir Technical University, Scientific Research Project Commission under grant number 19ADP079. We thank the METU Central Lab (Ankara/Turkey) for ICP-OES analyses, E. Ayas for SEM analyses, M. Tamer for TGA analyses, and D. Karabulut for helping with laboratory work.

## REFERENCES

- [1] K. Leng, Y. Wang, C. Hou, C. Lancelot, C. Lamonier, A. Rives, Y. Sun, *J. Catal.* 306 (2013) 100–108. <http://doi.org/10.1016/j.jcat.2013.06.004>.
- [2] N. Candu, M. Florea, S.M. Coman, V.I. Parvulescu, *Appl. Catal., A* 393 (2011) 206–214. <https://doi.org/10.1016/j.apcata.2010.11.044>.
- [3] D. Yin, C. Li, L. Tao, N. Yu, S. Hu, D. Yin, *J. Mol. Catal. A: Chem.* 245 (2006) 260–265. <https://doi.org/10.1016/j.molcata.2005.10.010>.
- [4] N. Candu, S. Wuttke, E. Kemnitz, S.M. Coman, V.I. Parvulescu, *Pure Appl. Chem.* 84 (2012) 427–437. <http://doi.org/10.1351/PAC-CON-11-09-34>.
- [5] K. Leng, S. Sun, B. Wang, L. Sun, W. Xu, Y. Sun, *Catal. Commun.* 28 (2012) 64–68. <https://doi.org/10.1016/j.catcom.2012.08.016>.
- [6] Y. Wang, Y. Sun, C. Lancelot, C. Lamonier, J.C. Morin, B. Revel, L. Delevoye, A. Rives, *Microporous Mesoporous Mater.* 206 (2015) 42–51. <http://doi.org/10.1016/j.micromeso.2014.12.017>.
- [7] V.D. Chaube, *Catal. Commun.* 5 (2004) 321–326. <https://doi.org/10.1016/j.catcom.2004.02.013>.
- [8] H. Jin, M.B. Ansari, E.Y. Jeong, S.E. Park, *J. Catal.* 291 (2012) 55–62. <https://doi.org/10.1016/j.jcat.2012.04.006>.
- [9] Y. Sun, R. Prins, *Appl. Catal., A* 336 (2008) 11–16. <https://doi.org/10.1016/j.apcata.2007.08.015>.
- [10] L. Tosheva, V.P. Valtchev, *Chem. Mater.* 17 (2005) 2494–2513. <https://doi.org/10.1021/cm047908z>.
- [11] J.C. Groen, J.A. Moulijn, J. Pérez-Ramírez, *J. Mater. Chem.* 16 (2006) 2121–2131. <https://doi.org/10.1039/B517510K>.
- [12] D. Verboekend, J. Pérez-Ramírez, *Catal. Sci. Technol.* 1 (2011) 879–890. <https://doi.org/10.1039/C1CY00150G>.
- [13] L. Wang, Y. Wang, A. Wang, X. Li, F. Zhou, Y. Hu, *Microporous Mesoporous Mater.* 180 (2013) 242–249. <http://doi.org/10.1016/j.micromeso.2013.06.029>.
- [14] C. Perego, S. Amarilli, R. Millini, G. Bellussi, G. Girotti, G. Terzoni, *Microporous Mater.* 6 (1996) 395–404. [https://doi.org/10.1016/0927-6513\(96\)00037-5](https://doi.org/10.1016/0927-6513(96)00037-5).
- [15] R. Millini, F. Frigerio, G. Bellussi, G. Pazzucconi, C. Perego, P. Pollesel, U. Romano, *J. Catal.* 217 (2003) 298–309. [https://doi.org/10.1016/S0021-9517\(03\)00071-X](https://doi.org/10.1016/S0021-9517(03)00071-X).
- [16] E.R. Rosinski, M.K. Rubin, US 3832449 (1974).
- [17] L.T. Nemeth, G.F. Maher, US 6872866B1 (2005).
- [18] B.H. Chiche, R. Dutartre, F. Di Renzo, F. Fajula, A. Katovic, A. Regina, G. Giordano, *Catal. Lett.* 31 (1995) 359–366. <https://doi.org/10.1007/BF00808600>.
- [19] S. Akyalcin, L. Akyalcin, M. Bjørgen, *Microporous Mesoporous Mater.* 273 (2019) 256–264. <https://doi.org/10.1016/j.micromeso.2018.07.014>.
- [20] S. Gopal, K. Yoo, P.G. Smirniotis, *Microporous Mesoporous Mater.* 49 (2001) 149–156. [https://doi.org/10.1016/S1387-1811\(01\)00412-7](https://doi.org/10.1016/S1387-1811(01)00412-7).
- [21] Y. Hou, N. Wang, J. Zhang, W. Qian, *RSC Adv.* 7 (2017) 14309–14313. <https://doi.org/10.1039/C6RA28844H>.
- [22] D. Karabulut, S. Akyalcin, *Int. J. Chem. React. Eng.* 19 (2021) 541–551. <https://doi.org/10.1515/ijcre-2020-0175>.
- [23] X. Wei, P.G. Smirniotis, *Microporous Mesoporous Mater.* 97 (2006) 97–106. <https://doi.org/10.1016/j.micromeso.2006.01.024>.
- [24] A.L. Patterson, *Phys. Rev.* 56 (1939) 978. <https://doi.org/10.1103/PhysRev.56.978>.
- [25] K.T.G. Carvalho, E.A. Urquieta-Gonzalez, *Catal. Today* 243 (2015) 92–102. <http://doi.org/10.1016/j.cattod.2014.09.025>.
- [26] K.S.W. Sing, D.H. Everett, R.A.W. Haul, L. Moscou, R.A. Pierotti, J. Rouquerol, T. Siemieniewska, *Pure Appl. Chem.* 57 (1985) 603–619.

- <http://doi.org/10.1351/pac198557040603>.
- [27] J.C. Groen, L.A.A. Peffer, J.A. Moulijn, J. Pérez-Ramírez, *Colloids Surf., A* 241 (2004) 53–58. <https://doi.org/10.1016/j.colsurfa.2004.04.012>.
- [28] J.C. Groen, J.C. Jansen, J.A. Moulijn, J. Pérez-Ramírez, *J. Phys. Chem. B* 108 (2004) 13062–13065. <https://doi.org/10.1021/jp047194f>.
- [29] Q. Wang, Z.M. Cui, C.Y. Cao, W.G. Song, *J. Phys. Chem. C* 115 (2011) 24987–24992. <https://doi.org/10.1021/jp209182u>.
- [30] U.V. Mentzel, K.T. Højholt, M.S. Holm, R. Fehrmann, P. Beato, *Appl. Catal., A* 417–418 (2012) 290–297. <https://doi.org/10.1016/j.apcata.2012.01.003>.
- [31] M. Bjørgen, F. Joensen, M. Spangsborg Holm, U. Olsbye, K. P. Lillerud, S. Svelle, *Appl. Catal., A* 345 (2008) 43–50. <https://doi.org/10.1016/j.apcata.2008.04.020>.
- [32] K. Sadowska, A. Wach, Z. Olejniczak, P. Kustrowski, J. Datka, *Microporous Mesoporous Mater.* 167 (2013) 82–88. <https://doi.org/10.1016/j.micromeso.2012.03.045>.
- [33] S.J. You, E.D. Park, *Microporous Mesoporous Mater.* 186 (2014) 121–129. <http://doi.org/10.1016/j.micromeso.2013.11.042>.
- [34] S. Svelle, L. Sommer, K. Barbera, P.N.R. Vennestrøm, U. Olsbye, K.P. Lillerud, S. Bordiga, Y.H. Pan, P. Beato, *Catal. Today* 168 (2011) 38–47. <https://doi.org/10.1016/j.cattod.2010.12.013>.
- [35] X. Zeng, Z. Wang, J. Ding, L. Wang, Y. Jiang, C. Stampfl, M. Hunger, J. Huang, *J. Catal.* 380 (2019) 9–20. <https://doi.org/10.1016/j.jcat.2019.09.035>.
- [36] M. Milina, S. Mitchell, Z.D. Trinidad, D. Verboekend, J. Pérez-Ramírez, *Catal. Sci. Technol.* 2 (2012) 759–766. <https://doi.org/10.1039/C2CY00456A>.
- [37] H.S. Fogler, *Elements of Chemical Reaction Engineering*, Prentice Hall, Englewood Cliffs, NJ, USA (1999). ISBN 0-13-531708-8.
- [38] N. Narender, K.V.V. Krishna Mohan, S.J. Kulkarni, I. Ajit Kumar Reddy, *Catal. Commun.* 7 (2006) 583–588. <https://doi.org/10.1016/j.catcom.2006.01.013>.
- [39] K. Yoo, P.G. Smirniotis, *Appl. Catal., A* 246 (2003) 243–251. [https://doi.org/10.1016/S0926-860X\(03\)00026-7](https://doi.org/10.1016/S0926-860X(03)00026-7).
- [40] J.C. Kim, K. Cho, R. Ryoo, *Appl. Catal., A* 470 (2014) 420–426. <https://doi.org/10.1016/j.apcata.2013.11.019>.
- [41] D.S.A. Silva, W.N. Castelblanco, D.H. Piva, V. Macedo, K.T.G. Carvalho, E.A. Urquieta-González, *Mol. Catal.* 492 (2020) 111026. <https://doi.org/10.1016/j.mcat.2020.111026>.
- [42] J. Shao, T. Fu, Z. Ma, C. Zhang, H. Li, L. Cui, Z. Li, *Catal. Sci. Technol.* 9 (2019) 6647–6658. <https://doi.org/10.1039/C9CY01053J>.
- [43] G. Cruciani, *J. Phys. Chem. Solids* 67 (2006) 1973–1994. <https://doi.org/10.1016/j.jpcs.2006.05.057>.

SEMA AKYALCIN<sup>1</sup>  
LEVENT AKYALCIN<sup>1</sup>  
MORTEN BJØRGEN<sup>2</sup>

<sup>1</sup>Department of Chemical Engineering, Faculty of Engineering, Eskisehir Technical University, Eskisehir, Turkey

<sup>2</sup>Department of Life Sciences and Health, Faculty of Health Sciences, Oslo Metropolitan University, Oslo, Norway

## KATALITIČKA SVOJSTVA DESILIKOVANOG ZEOLITA HZSM-12 ZA REAKCIJU BENZILOVANJA BENZENA SA BENZIL ALKOHOLOM

*Katalitička proizvodnja difenilmetana u reakciji benzena sa benzil alkoholom je istraživana korišćenjem HZSM-12 i desilikovanog HZSM-12 koji je dobijen tretiranjem ZSM-12 sa 0,2M NaOH na 85 °C tokom 60 min. Netretirani i alkalno tretirani zeoliti ZSM-12 su okarakterisani rendgenskom difrakcijom, izotermama adsorpcije/desorpcije azota, skenirajućom elektronskom mikroskopom, optičkom emisionom spektrometrijom induktivno spregnute plazme i temperaturno programiranom desorpcijom amonijaka. Desilikovani HZSM-12 ima dobra katalitička svojstva za konverziju benzil-alkohola od 100% i selektivnost prema difenilmetanu od 74% i 87% (za 4 h i 8 h reakcionog vremena, redom). Prikazani su, takođe, reakcioni parametri koji utiču na konverziju benzil-alkohola i distribuciju proizvoda. Upoređene su aktivnosti svežeg i regenerisanog katalizatora, a rezultati karakterizacije su pokazali da okludirani organski molekuli smanjuju broj kiselih mesta katalizatora nakon reakcije i regeneracije.*

*Ključne reči: benzil-alkohol, benzilovanje, deaktivacija katalizatora, desilikacija, difenilmetan, ZSM-12.*

NAUČNI RAD